# Analysis of High Manganese Stainless Steel Weldability Problem

*Emission spectroscopic techniques are applied to the study of penetration anomalies in GTA welding of 21Cr-6Ni-9Mn stainless steel*

BY G. S. MILLS

ABSTRACT. The emission spectroscopic techniques presented in a previous paper[2] are applied to the study of weldability problems encountered in GTA welding of high manganese austenitic stainless steels. It is found that variations in depth-to-width ratios, from one heat of steel to another of the same nominal composition (21%Cr-6%Ni-9%Mn), do not result from changes in heat flow in the arc. Instead, the data indicate that variations are related to differences in heat flow within the molten pool as evidenced by differences in the rate of evaporation of manganese from the pool surface.

## Introduction

A previous study[1] of the GTA (gas tungsten arc) weldability of a high manganese austenitic stainless steel (nominal composition 21%Cr-6%Ni-9%Mn) indicated that the depth-to-width ratio (D/W) of the fusion zone was related to aluminum content; an increase in aluminum content corresponding to a decrease in D/W. In addition, there was a strong increase in manganese spectral emission from the arc immediately above the pool on low D/W heats of steel. The relationship between these various aspects of the welding behavior of this steel was not understood at that time. In particular, it was not known whether the lower D/W was due to spreading of heat input from the arc or some arc-independent mechanism within the liquid pool.

A quantitative study of arc characteristics, using the techniques described in a previous article[2] was undertaken to determine their relationship to D/W explicitly. The results of this study and the conclusions drawn are reported here.

**Table 1—Arc Operating Conditions**

| | |
|---|---|
| Weld current | 100 A, DCSP |
| Electrode type | EWTh-2; 3/32 in. diam |
| Electrode gap | 0.06 in. |
| Torch gas | 20 cfh argon |
| Welding speed | 5 ipm |

**Table 2—Aluminum Contents and Values of Depth-to-Width Ratio (D/W)**

| Plate No. | Al (ppm) | D/W |
|---|---|---|
| 3231 | 20-30 | 0.40 |
| 4229 | 80-120 | 0.33 |
| 4235 | 300 | 0.22 |

## Experimental Procedures

Argon or manganese emission line intensities were measured as arcs that were run on rotating bar samples under the conditions given in Table 1. Meaningful measurements could be made only as the arc traversed fresh material at a rate similar to that used in production welding because evaporative transfer from the weld pool caused changes in composition, especially in the case of manganese. An additional difficulty was encountered in the case of this high manganese steel (particularly the high aluminum heats) in that the manganese vapor interfered with the argon plasma except in the immediate vicinity of the tungsten electrode.

As a result, attention was focused on determining temperature profiles from manganese line intensity measurements in the region of the arc immediately above the weld pool. Details of the measurement method and the calculation of plasma temperatures from the line intensities were given previously.[2]

## Results and Discussion

Because the techniques applicable to the argon plasma could be used only near the tungsten electrode, the few measurements made in this region were primarily sensitive to electrode shape and distance of the measurement from the electrode. The latter dependence yielded a sensitivity to arc length when measurements were made at a fixed point above the weld pool. Consistent measurements from heat to heat were prevented by the variable cooling effect of the manganese vapor.

Measurements of temperature profiles in the manganese plasma immediately above the weld pool yielded very definite variations with the different heats of steel. Various examples of the intensity and temperature profiles obtained are shown in Figs. 1 through 5.

Table 2 presents the aluminum contents and representative values of D/W. Note that the samples are labeled by plate number rather than heat number as by Bennett and Mills.[1] This was done because continuing studies of aluminum content versus welding behavior have shown that there is significant segregation of

*G. S. MILLS is with Rockwell International, Atomics International Division, Rocky Flats Plant, Golden, Colorado.*

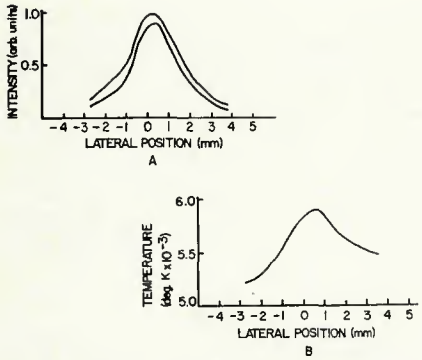


*Fig. 1—Intensity profiles of the 5341 (upper) and 5377 (lower) angstrom lines of manganese (A); temperature profile calculated from the ratio of intensities (B). Plate number 3231*

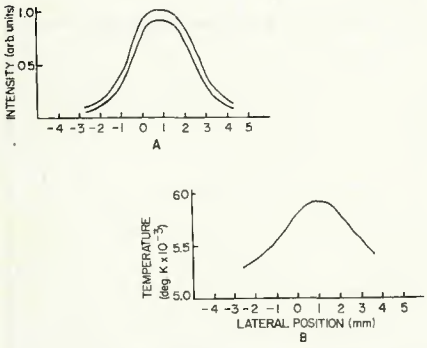


*Fig. 2—Intensity profiles of the 5341 (upper) and 5377 (lower) angstrom lines of manganese (A); temperature profile calculated from the ratio of intensities (B). Plate number 3231*

aluminum within individual ESR (electroslag remelt) ingots. Plate number 3231 is from heat number 81143 of reference 1 (vacuum arc remelt). The other two plates are from the same electroslag refined ingot (received after work in reference 1).

Comparing Fig. 1 with Fig. 2, and Fig. 3 with Fig. 4, gives an indication of the extent of intensity variations which result from the fluctuating conditions in these arcs. The arc corresponding to Fig. 5 was exceptionally stable. Such

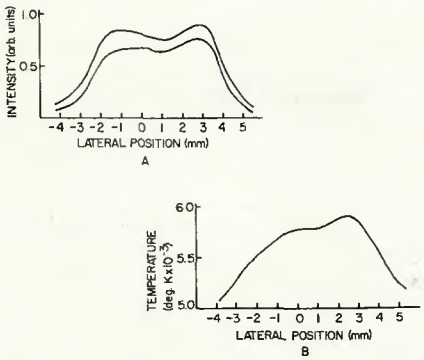


*Fig. 3—Intensity profiles of the 5341 (upper) and 5377 (lower) angstrom lines of manganese (A); temperature profile calculated from the ratio of intensities (B). Plate number 4229*

fluctuations do not have a gross effect on the weld because they are generally very rapid (many within one second), and their effect is averaged out to give a weld bead of uniform width. The shapes of the temperature profiles in the first two figures (peaked in the center) imply a more concentrated heat input than those in the next two figures (broad, relatively flat tops), in good agreement with their D/W values.

However, the temperature profile in Fig. 5 (again peaked in the center) would seem to indicate better weld behavior for plate number 4235 than for number 4229. This is not the case, as is clear from Table 2. The lack of consistent correlation between evident changes in temperature profiles and welding behavior raised the suspicion that the changes in D/W were not related to changes in arc temperature distribution. If the latter were the case, there had to be some explanation for the observed partial correlation (plates 3231 and 4229).

In an effort to explain the experimentally observed changes, temperature profiles were calculated from assumed radial distributions of temperature and gas density (using the

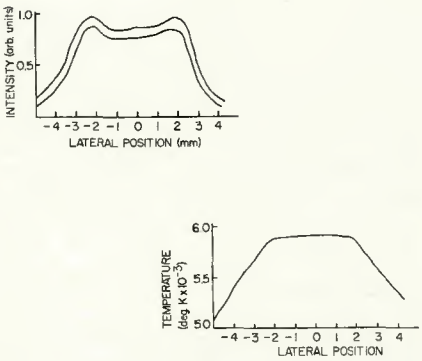


*Fig. 4—Intensity profiles of the 5341 (upper) and 5377 (lower) angstrom lines of manganese (A); temperature profile calculated from the ratio of intensities (B). Plate number 4229*

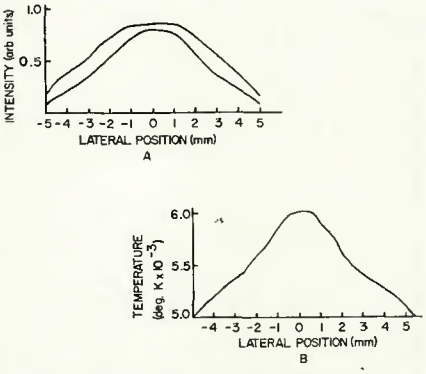


*Fig. 5—Intensity profiles of the 5341 (upper) and 5377 (lower) angstrom lines of manganese (A); temperature profile calculated from the ratio of intensities (B). Plate number 4235*

method outlined in Appendix B of reference 2). Plots of these profiles are shown in Figs. 6 and 8. It is clear that the distortions in the intensity profiles, induced by large changes in the density distribution, carry over into the temperature profiles.

Conceptually, the radial temperature distribution could be obtained again from the intensity profiles using the inversion method outlined in

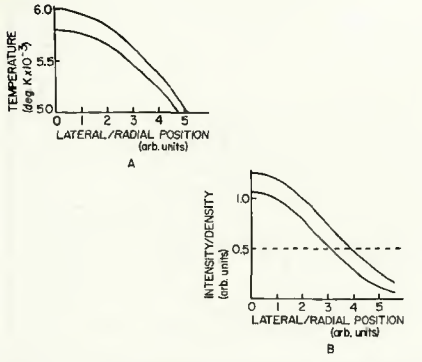


*Fig. 6—Assumed radial temperature distribution (upper) and calculated temperature profile (A); calculated intensity profiles (solid lines) and assumed relative radial density distribution (B)*

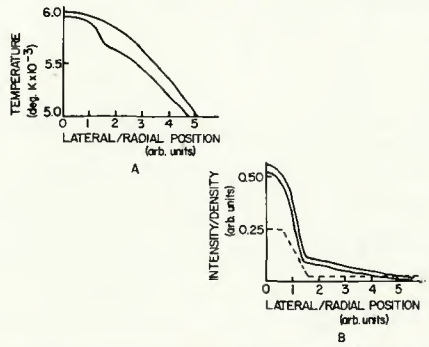


*Fig. 7—Assumed radial temperature distribution (upper) and calculated temperature profile (A); calculated intensity profiles (solid lines) and assumed relative radial density distribution (B)*

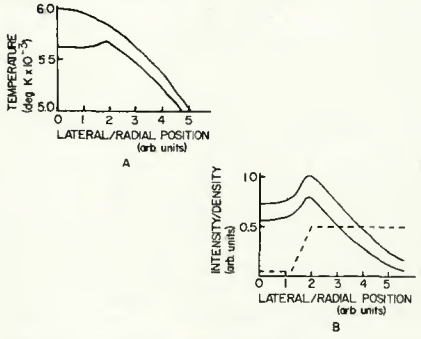


*Fig. 8—Assumed radial temperature distribution (upper) and calculated temperature profile (A); calculated intensity profiles (solid lines) and assumed relative radial density distribution (B)*

Appendix A of reference 2. However, this cannot be done with the experimental profiles because of errors introduced by fluctuations of the arc and the lack of circular symmetry. The latter problem is not eliminated by averaging because of the temperature gradients resulting from motion of the arc along a weld.

## Conclusion

The calculated temperature profiles (Figs. 7 and 8) could be made to simulate the major features of the experimental profiles shown in Figs. 1 through 4 by altering the density distribution alone (same radial temperature distribution). This suggests that the arc temperature distributions (heat flows) are the same from sample to sample except for secondary effects resulting from changes in the manganese vapor density distribution.

The vapor density above the pool is strongly related to the temperature and liquid manganese density distributions at the pool surface. Therefore, the strong variations in vapor density distribution resulting from the calculations simulating experimental profiles, also imply significant differences in heat (and material) flow within the pool.

These deductions concerning heat flow in the arc and the liquid pool lead to the conclusion that the observed changes in D/W result from changes in heat flow distribution in the liquid pool, not the arc. The mechanism which controls heat and material flow within the pool and its relationship to aluminum content is the subject of continuing studies.

*Acknowledgment*

This work was performed under a contract with the U.S. Energy Research and Development Administration.

*References*

1. Bennett, W. S., and Mills, G. S., "GTA Weldability Studies on High Manganese Stainless Steel," *Welding Journal*, 53 (12), Dec. 1974, Res. Suppl., pp. 549-s to 553-s.

2. Mills, G. S., "Use of Emission Spectroscopy for Welding Arc Analysis," *Welding Journal*, 56 (3), March 1977, Res. Suppl., pp. 93-s to 96-s.